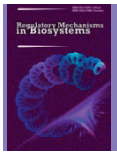

Regulatory Mechanisms in Biosystems

ISSN 2519-8521 (Print)
ISSN 2520-2588 (Online)
Regul. Mech. Biosyst.

Synthesis and characterization of Aspartame and Neotame-encapsulated PLGA-TPGS nanoparticles and their modulatory effects on acetylcholinesterase gene expression in male rats

A. J. Mohammed, H. K. Al-Awadi, H. H. K. Al-Shukri

Al-Qasim Green University, Babylon, Iraq

Article info

Received 15.04.2025
Received in revised form 27.05.2025
Accepted 21.06.2025

Veterinary Medicine College, Al-Qasim Green University, Babylon, 51013, Iraq.
E-mail: hamza14shukri72@gmail.com

Mohammed, A. J., Al-Awadi, H. K., & Al-Shukri, H. H. K. (2025). Synthesis and characterization of Aspartame and Neotame-encapsulated PLGA-TPGS nanoparticles and their modulatory effects on acetylcholinesterase gene expression in male rats. Regulatory Mechanisms in Biosystems, 16(2), e25067. doi:10.15421/0225067

This study investigates the synthesis, characterization, and biological impact of novel nanoparticle formulations of two artificial sweeteners Aspartame and Neotame encapsulated in PLGA-TPGS (poly(lactic-co-glycolic acid)-D-α-tocopheryl polyethylene glycol 1000 succinate) matrices. Nanoparticles were developed using a combination of emulsification, sonication, and solvent evaporation techniques, followed by detailed physicochemical characterization via UV–Vis spectroscopy, SEM, TEM, DLS, FTIR, and EDX. The *in vitro* release profiles demonstrated sustained release patterns for both Aspartame (ASPNPs) and Neotame (NEONPs) formulations compared to their free forms. *In vivo* experiments using male Wistar rats assessed the effects of these sweeteners and their nanoformulations on acetylcholinesterase (AChE) gene expression. Free forms of Aspartame and Neotame significantly elevated AChE gene expression, suggesting potential neurotoxic effects, while ASPNPs and NEONPs mitigated this elevation, indicating a protective role of nanoencapsulation. These findings highlight the potential of PLGA-TPGS nanoparticle systems in reducing the neurotoxic effects associated with chronic intake of synthetic sweeteners through controlled release and improved bioavailability.

Keywords: Aspartame; Neotame; PLGA-TPGS nanoparticles; acetylcholinesterase; neurotoxicity; gene expression; controlled release.

Introduction

Artificial sweeteners, also known as low-calorie sweeteners (LCS) or non-nutritive sweeteners (NNAS), are becoming more and more common in contemporary diets as a low-calorie substitute for sugar in a variety of food and drink items. About 150 years after saccharin was first synthesized, a number of artificial sweeteners with distinct qualities and applications are currently being made. Aspartame is a low-calorie, non-nutritive artificial sweetener advertised as 'Diet Sweet' and is approximately 200 times as sweet as sucrose (Samreen & Dhaneshwar, 2023). Because of its various benefits, including its low-calorie content, suggested body weight management, and lower costs, it is gaining popularity. Additionally, it became more well-known in as an alternativet to consuming sugar (Mora & Dando, 2021). Aspartame has expanded widely and been added to foods including soft drinks, candies, chewing gum, syrups, mouth fresheners, and gelatins. It is now advised for weight loss and for those with type 2 diabetes (Schorb et al., 2023). Since Aspartame is an ingredient in many items, adults and children may inadvertently ingest higher doses than the FDA recommends, which could have major negative health effects. Aspartame-containing foods need to be marked with the words "contains phenylalanine." Furthermore, items containing Aspartame must be labeled to state that baking and cooking are not advised. Even though Aspartame's health consequences have been the subject of much research, its usage in food and pharmaceutical goods is still debatable and its long-term effects are hard to predict (Czarnecka et al., 2021). When Aspartame ingested, it is completely metabolized by the gut enzymes (peptidase and esterase) into three main components phenylalanine (Phe) (50%), aspartic acid (aspartate) (40%), and methanol (MeOH) (10%) (Farag et al., 2022).

Neotame is formed when the tertiary butyl group is added to amine free group of aspartic acid (Farag et al., 2022). Neotame, (3 S)-3-(3,3-dimethylbutylamino)-4-[(2 S)-1-methoxy-1-oxo-3-phenylpropan-2-yl amino]-4-oxobutanoic acid is an artificial sweetener and chemically synthesized from Aspartame. It has similar physical properties as Aspartame in terms of sweetness and comparable with sucrose without a metallic or bitter after taste at high concentrations (Ruiz-Ojeda et al., 2019).

Neotame was permitted for use by the FDA in 2002, but still it is hardly used. Studies revealed that Neotame affects body weight. These effects are not due to the toxic nature of Neotame, instead they relate to the indigestibility of foods containing Neotame as e sweetener. Due to this reason, animal models showed less weight gain or loss in body weight on long-term exposure to Neotame (Silva et al., 2023).

Nanoparticles are tiny particles with sizes ranging from one to one hundred nanometers. They differ greatly from their larger counterparts in terms of their physical and chemical characteristics because of their minuscule size. As they go closer to the atomic scale, these characteristics alter, and the material's performance is dominated by its surface atoms (Joudeh & Linke, 2022). Particulate dispersions or solid particles with a size between 10 and 1000 nm are referred to as nanoparticles. The medication is encapsulated, dissolved, trapped, or bonded to a matrix of nanoparticles. Nanospheres and nanocapsules are produced based on the preparation techniques decribed by Ali et al. (2023). There are various applications such as: air purification, cosmetics, healthcare, environmental protection and many others which utilize nanotechnologies. Brushes paints, plastics and even ceramics contain industrial nanoparticles, which worsens pollution (Khan et al., 2022). One of the focus areas is tailoring designable features into nanoparticles in nanotechnology (Chauhan et al., 2022).

Poly-lactic-co-glycolic acid (PLGA) is one of the most widely used polymers for drug delivery systems in biomedicine, due to its biodegradability, biosafety, biocompatibility and versatility in formulation and functionalization (Lu et al. 2023). PLGA was synthesized through a catalyst-mediated random ring-opening copolymerization of lactic acid and glycolic acid which results in an ester linkage between both polymers. Alvi et al. (2022) documented that both component polymers are metabolized by the Krebs cycle and ultimately converted to pyruvate. PLGA-NPs enter the cell partly through fluid-phase pinocytosis, and the remainder enters the cell via clathrin-coated pits present in vascular smooth muscle cells (VSMCs) (Sahoo et al., 2024). The blood half-life of NPs can especially be increased by combining PLGA with other polymers like polyethylene glycol (PEG), polyvinyl alcohol (PVA), and D-α-tocopheryl PEG 1000 succinate (TPGS) (Shah et al., 2024).

Dopamine, or 3-hydroxytyramine, is an endogenous catecholamine that is important to both neuronal and nonneuronal processes. Dopamine was first synthesized in 1910, and initial studies examined its biological effect as a weak sympathomimetic, although the mechanism of action was not clear (Riederer & Horowski, 2023). Dopamine primarily mediates its effects on different cell types by signaling through dopamine receptors, which are G-protein coupled receptors (GPCRs). Paul Greengard and colleagues defined two distinct signaling pathways that activate or inhibit the ubiquitous second messenger 3′-5′ cAMP and are mediated by different types of dopamine receptors (Preto et al., 2020). Nitric oxide (NO) is a ubiquitous gaseous molecule that is water soluble and can pass freely across cell membranes. It has a free radical structure making it notoriously noxious and possesses an extra electron, which allows it to be highly reactive (Andrabi et al., 2023). Endogenous NO serves as an important effector and signal transduction molecule in numerous cellular processes involved in physiological states such as vasodilation, immune responses, neurotransmission, apoptosis, reproduction, regulation of gene transcription, mRNA translation, and post-translational modifications of proteins (Ngo & Duennwald, 2022).

Glial fibrillary acidic protein (GFAP) is the main intermediate filament (IF) protein in mature astrocytes of the central nervous system (CNS). It is also an important component of the astrocyte cytoskeleton during development. The structural role of GFAP in astrocytes is well-accepted. However, over the years, it has become evident that GFAP is involved in significant astrocyte functions during regeneration, synaptic plasticity, and reactive glial encapsulation. Furthermore, different astrocyte subpopulations, likely having distinct roles in brain physiology and pathology, are categorized not only by their spatial and temporal occurrence but also by their specific expression of IFs, including distinct GFAP isoforms. The existence of these isoforms adds complexity to the astrocyte cytoskeleton and likely underlies specific subtype functions.(Middeldorp & Hol, 2011; Jurga et al., 2021).

Acetylcholine (cholinergic neurotransmitter, ACh) is an excitatory neurotransmitter secreted by presynaptic neurons in the synaptic cleft both in the PNS and CNS. They are also released in the neuromuscular junctions involving neurons and muscle cells (Sam & Bordoni, 2020). The biosynthesis of acetylcholine in the acetylcholinergic neurons commences from amino acid Ser. It later undergoes decarboxylation in the presence of the enzyme serine decarboxylase to form the β-aminoethanol called choline. Acetylcholinesterase (AChE) is the essential enzyme in the serine hydrolases family in cholinergic synapses that plays a crucial role in memory and cognition. AChE is responsible for hydrolysis of the neurotransmitter acetylcholine (ACh) into choline and acetate at cholinergic synapses, terminating synaptic transmission (Jovičić, 2024). This study aims to synthesize, characterize, and study the effects of the artificial sweeteners Aspartame and Neotame-PLGA-TPGS nanoparticles (ASNPs and NEONPs) on the acetylcholine esterase gene expression in male rats.

Materials and methods

We certify that this research complied with ethical standards, following the Helsinki Declaration (1975, revised in 2013) and relevant national regulations and approved by ethical committee in Al-Qasim Green University No. 223 at 20-3-2024.

Fifty male Wister rats were randomly assigned to five groups for this investigation, with 10 animals in each group: the control group (CONT), the Aspartame group (ASP), the Neotame group (NEO), the Aspartame nanoparticles (ASPNPs) and the Neotame nanoparticles group (NEONPs). The following are groups of experiments, Group 1 (CONT): 8 weeks of regular tap water administration. For eight weeks, Group 2 (ASP) received 500 mg/kg of Aspartame per day dissolved in tap water (Magnuson et al., 2007). For eight weeks, Group 3 (NEO) received 500 mg/kg of Neotame per day dissolved in tap water (Chi et al., 2018). Group 4 (ASPNPs): 500 mg/kg/day of ASPNPs dissolved in drinking water for eight weeks. Group 5 (NEONPs): 500 mg/kg/day of NEONPs dissolved in tap water for eight weeks.

Sonication, emulsification/solvent evaporation, and, with minor adjustments, the ionic gelation process were used to create (ASPNPs) (Aspartame loaded PLGA NPs). The possible mechanism for ionic gelation is that the ionic interaction between positively charged Aspartame with negatively charged tocopherol polyethylene glycol succinate (TPGs).

The summary of the protocol that used in Aspartame-PLGA-TPGS NPs preparation is illustrate in the following steps:

1. Using a stirrer, we vibrated 500 mg of Aspartame in 100 mL of deionized cold water until it was fully dissolved.

2. PLGA 0.250 mg was dissolved using a stirrer in 20 mL of dichloromethane (DCM).

3. 0.1 mg of TPG leaves was dissolved in D.D.W., 10 mL of deionized distilled water was poured into a plastic tube and left overnight.

4. An solution is created by combining steps one and two, and it is then gradually added to the organic face (TPGS solution) via burette for 30 minutes.

5. Using an ultrasonic probe sonication, the produced solution was combined to create an emulsion of nanoparticles. To get rid of the chloroform and prevent the development of nanoparticles, the emulsion was agitated all night. To get rid of bigger particles, the prepared nanoparticles were centrifuged for 10 minutes at 4,000 rpm.

6. The centrifugation was again done for 15 min at 12,000 rpm, and the clear supernatant was removed, and settled nanoparticles were washed with distilled water to remove the excess particles that adhered to the surface of nanoparticles. A dispersion of resulting nanoparticles in distilled water was made by using vortex.

7. Nanoparticles that were prepared by the above procedure were sent to a special nanotechnology laboratory for nanoparticle characterization.

For preparation of NEONPs, the same above steps were taken but we used Neotame instead of Aspartame to form of NEONPs.

Following their dissolution in 2% (v/v) glacial acetic acid, the produced ASPNPs and NEONPs were scanned using a Shimadzu spectrophotometer (Model UV-1800 Japan) set to operate at a resolution of 1 nm in the UV-visible spectrum. Patterns of ASPNPs and NEONPs were analyzed using Energy Dispersive X-ray Spectroscopy (EDX). To estimate the sizes and charges of the nanoparticles, the ASPN Ps and NEONPs' partial sizes (PS), polydispersity index (PDI), and zeta potential (ZP) values were evaluated. The morphological characteristics of the produced Aspartame-PLGA-TPGS (ASPNPs) and Neotame-PLGA-TPGS (NEONPs) nanoparticles were well illustrated by the SEM and TEM examination.

The surface topography and particle morphology of the prepared nanoparticles (ASPNPs and NEONPs) were analyzed by Scanning Electron Microscopy (SEM) analysis. A small of amount of lyophilized nanoparticles was sprinkled on a double-sided carbon adhesive tape glued to an aluminum stub. The samples were sputter coated under vacuum with a thin layer of gold (sputter coater, Quorum Q150R ES, UK) to improve conductivity.

TEM analysis was used to further investigate the internal structure, morphology and particle size of the nanoparticles. Ultra-sonication was used to make dilute suspension (in distilled water) of ASPNPs and NEONPs in order to avoid aggregation. A drop of the suspension was disposed on a carbon-coated copper grid (200 mesh) and left to stand for 1–2 min, and then the extra fluid was adsorbed away with a filter paper. Grids were air-dried at room temperature and observed in a TEM (JEOL JEM-2100, Japan) operating at 120 kV.

The particle sizes distribution (hydrodynamic diameter), polydispersity index (PDI) and zeta potential of the obtained ASPNPs and NEONPs were determined by using a Dynamic Light Scattering (DLS) kit (e.g., Malvern Zetasizer Nano ZS, UK). The nanoparticles were uniformly dispersed in deionised water and sonicated for 5 minutes to prevent aggregation prior to the measurement. Samples were placed in one-use disposable polystyrene cuvettes (for size and PDI) or folded capillary cells (for zeta potential). Measurements were performed in triplicate at 25°C and data was presented as the mean ± SD. The PDI values served to quantify the homogeneity of the nanoparticle dispersion.

The possible chemical interactions between Aspartame and Neotame with PLGA-TPGS nanoparticles and the encapsulation of the

agents in PLGA-TPGS-nanoparticles were studied using Fourier Transform Infrared Spectroscopy (FTIR). FTIR spectra of Aspartame pure drug (ASP), Neotame (NEO) pure drug, along with PLGA, TPGS, physical mixtures (drug + polymers) and the prepared developed nanoparticles (ASPNPs and NEONPs) were obtained by carrying out the KBr disc method using a FTIR spectrometer (e.g., PerkinElmer Spectrum Two, USA). About 2.0 mg of each sample was ground to a fine powder and mixed with dry potassium bromide (KBr) powder in a ratio of 1:100 (w/w); the mixture was compressed into transparent pellets with a hydraulic press (Proetractor-Type Niemi cylinder) of 8-ton pressure for 5 min. The experiments were performed and the full midIR spectra were collected from 4000 to 400 cm^{-1} in transmission mode at a resolution of 4 cm^{-1} averaged over 32 scans to improve the signal-to-noise ratio. The FTIR analysis was performed to recognize the functional group characteristic peaks in the Aspartame and Neotame and to find out whether there was any change in the peak position, or disappearance or appearance of new peaks in the nanoparticle formulations that reflect drug-polymer interaction, or successful encapsulation of the drug. Special attention was focused on the amine ($–NH_2$), carbonyl (C=O), ester (–COO–), and hydroxyl (–OH) group peaks.

A beaker with 200 mL of release medium (PBS pH 7.4) was filled with a dialysis bag (12000 Da) with a surface area of 17.58 ± 1.15 cm^2 that contained 5 mL of either ASP-loaded NPs suspension (5 mg/mL) or non-encapsulated drug solution (free ASP). Throughout the experiment (about 100 hours), the systems were kept at 37 °C with continuous magnetic stirring (300 xg). At preselected time intervals, 3 mL of the release media was taken out and centrifuged (6000 g) to collect the supernatant. To the pellet containing NPs with unreleased ASP, an equal volume of fresh media was added (3 mL DW was added to replace 3 mL that taken). The samples were filtered through a 0.45 µm PVDF membrane (Millipore®). The collected supernatants containing released ASP were then analyzed by spectrophotometer. The ASP release % at sample time was calculated for free ASP and ASPNPs formulations depending on the following equation:

ASP release (%) = (Amount of ASP released at time t /
/ Total amount of ASP in the formulation) * 100

In vitro Neotame release profile (NEO release %) was performed by repeating the same steps for Aspartame release analysis but using of NEO instead of ASP.

Determination of rat DRD1 (Dopamine Receptor D1 Rat NO (nitric oxide), and rat GFAP (Glial Fibrillary Acidic Protein) were performed by used the sandwich ELISA kits depending on the instructions of the manufacturer.

Using the Trizol Up RNA Kit, genomic RNA was isolated from blood by following the instructions on the RNA extraction kit.

As indicated in Table 1, the primer sequence for rat AChE gene expression utilized in this investigation was supplied by Macrogen Company, Korea.

PCR master mix for was prepared by using (Promega Master Mix kit) and this master mix was made according to company instructions as following Table 2. PCR thermo cycler conditions were created by using a Real time PCR thermocycler system as shown in Table 3.

Table 1
The PCR Primers with their sequence

Primers		Sequence	Amplicon length, bp	Reference
AChE-mRNA	F	5-ACACCGTGGAGGAGAGAATC-3	300	Padhi et al. (2020)
	R	5-TCTCTOCOGTCCTTOCAAC-3		
GAPDH	F	5-AGTTCAACGGCACAGTCAAG-3	120	
	R	5-CATACTCAGCACCAGCATCAC -3		

Statistical analysis of the obtained experimental data qRT-PCR regarding the target gene and reference gene was performed through determining the fold change test that relies on relative quantification of expression level of the gene. The relative expression of rat AChE gene was calculated using the $2^{-\Delta\Delta Ct}$ method (Işık & Beydemir, 2022). We also calculated the CT value of the reference gene against that of the target gene using the subsequent formulae:

$$\Delta CT\ (Test) = CT\ (ref,\ test) - CT\ (target,\ test),$$
$$\Delta\Delta CT = \Delta CT\ (test) - \Delta CT\ (control),$$

where ΔCT: CT of target – CT of actin.

$$\text{Fold change expression (FCE)} = 2^{-\Delta\Delta CT}$$

The ratio (reference to target) was calculated using the 2CT (reference) − CT (target) formula.

Table 2
PCR Master Mix preparation

Master Mix	Volume, µL
GoTaq® qPCR Master Mix, 2X	10
Forward Primer, 10X	2
Reverse Primer, 10X	2
GoScript™ RT Mix for 1-Step RT-qPCR	0.4
RNA Template	4
Nuclease-Free Water to	20

Table 3
PCR Thermocycle conditions

Stage	Repeat	Temperature and time
Reverse transcription	1	≥37 °C for 15 minutes
RT inactivation/Hot-start activation	1	95 °C for 10 minutes
3-Step qPCR:		
a. Denaturation	40	95 °C for 10 seconds 61 °C
b. Annealling		for 30 seconds 72 °C for
c. Extension		30 seconds
Dissociation	1	60–95 °C

The statistical program Graphpad Prism for Windows, version 6.0, will be used for statistical analysis. The means ± SD (standard deviation) is used to display the data. Turkey's post-hoc test is used to account for multiple comparison treatments after the one-way analysis of variance (one-way ANOVA) is used to statistically evaluate the effects of treatments. Statistical significance is determined at the level $P < 0.05$.

Results and discussion

As seen in Figures 1 and 2, the current study's recorded UV-visible spectra revealed an absorption peak at 224 and 202 nm, respectively, which correspond to the p-p* transition of the ASPNPs and NEONPs. TEM investigation clearly demonstrated the spherical morphology of ASPNPs, which primarily ranged in size from 60 to 240 nm. The results also showed that the UV–Vis absorbance peak appeared around 224-331 nm for ASPNPs and in the range between 202–963 nm for NEONPs (Fig. 1 and 2). The absorption spectrum of UV-VIS of ASPNPs and NEONPs were performed through UV-VIS spectrophotometry, which was utilized to examine the creation and durability of ASP and NEO nanoparticles within the colloidal solution at varying time intervals of irradiation.

UV-visible spectroscopy serves as a rapid, simple, and reliable primary characterization technique for nanoparticles, particularly for monitoring the synthesis and stability of metal nanoparticles (Ronavari et al., 2021; Rahuman et al., 2022; Nkosi et al., 2024). The technique makes use of the special optical properties of nanoparticles, particularly their ability to react to particular light wavelengths (Bamal et al., 2021). This interaction produces a characteristic surface plasmon resonance (SPR) band for metal nanoparticles, like silver particles, which forms approximately between 400 and 450 nm for silver nanoparticles and between 500 and 550 nm for gold nanoparticles (Ronavari et al., 2021).

The Energy Dispersive X-ray Spectroscopy (EDX) analysis patterns of ASPNPs and NEONPs are displayed in Figures 3 and 4.

The EDX analysis for Aspartame-PLGA-TPGS nanoparticles (ASPNPs) and Neotame-PLGA-TPGS nanoparticles (NEONPs) provides an important understanding regarding the composition and surface chemistry of the sample. EDS test provided both qualitative and quantitative analysis of elements such as carbon, oxygen, nitrogen that might be involved in the formation of nanoplates and sulfur (Amaliyah et al., 2020). ASPNPs and NEONPs were found to be pure where C and O were major elements detected in the prepared nano formulations and carbon atoms were obtained in the highest amount.

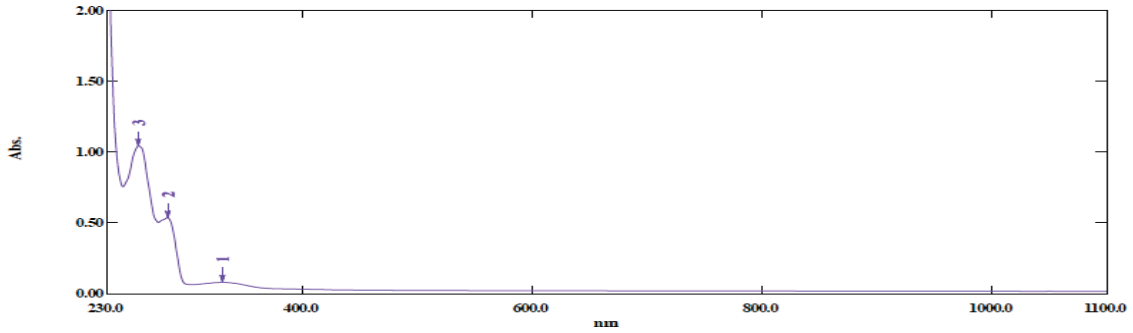

Threshold: 0.001
Number of Points: 8

No.	P/V	Wavelength nm.	Abs.	Description
1	↑	331.0	0.076	
2	↑	283.0	0.534	
3	↑	258.0	1.043	
4	↑	224.0	3.858	

Fig. 1. UV–Visible spectrum of ASPNPs

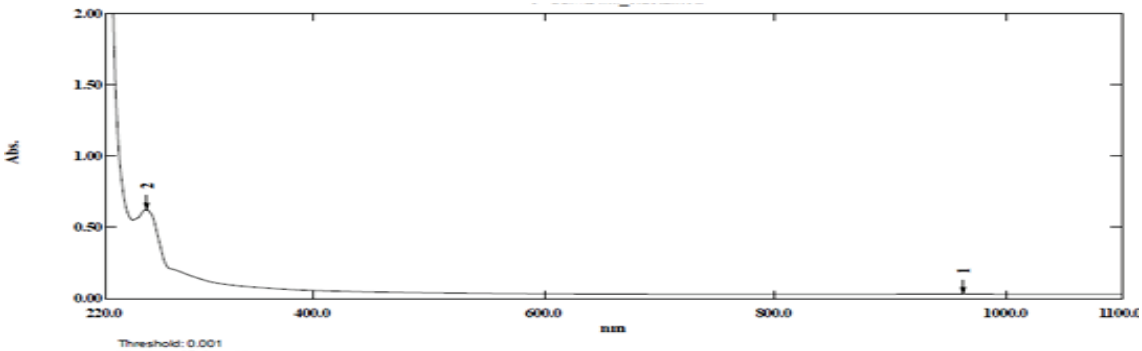

Threshold: 0.001
Number of Points: 11

No.	P/V	Wavelength nm.	Abs.	Description
1	↑	963.0	0.028	
2	↑	256.0	0.619	
3	↑	202.0	3.696	

Fig. 2. UV–Visible spectrum of NEONPs

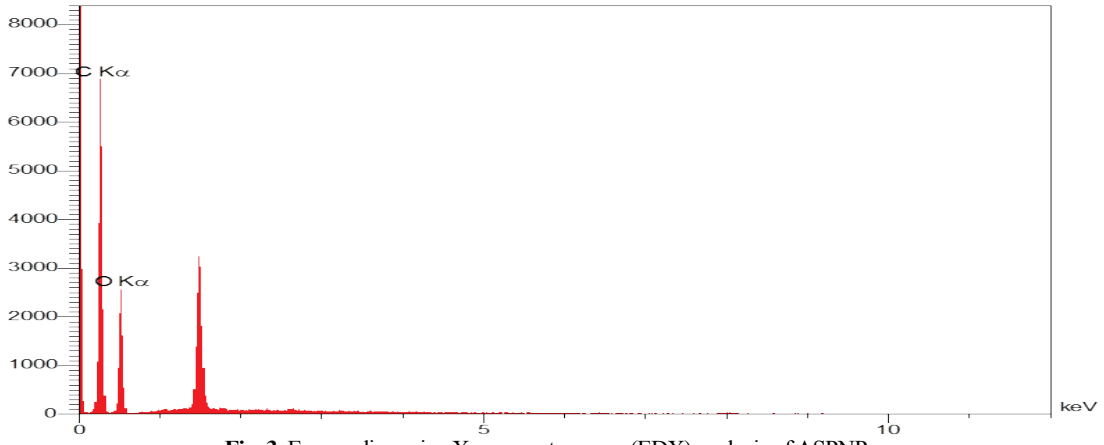

Fig. 3. Energy dispersive X-ray spectroscopy (EDX) analysis of ASPNPs

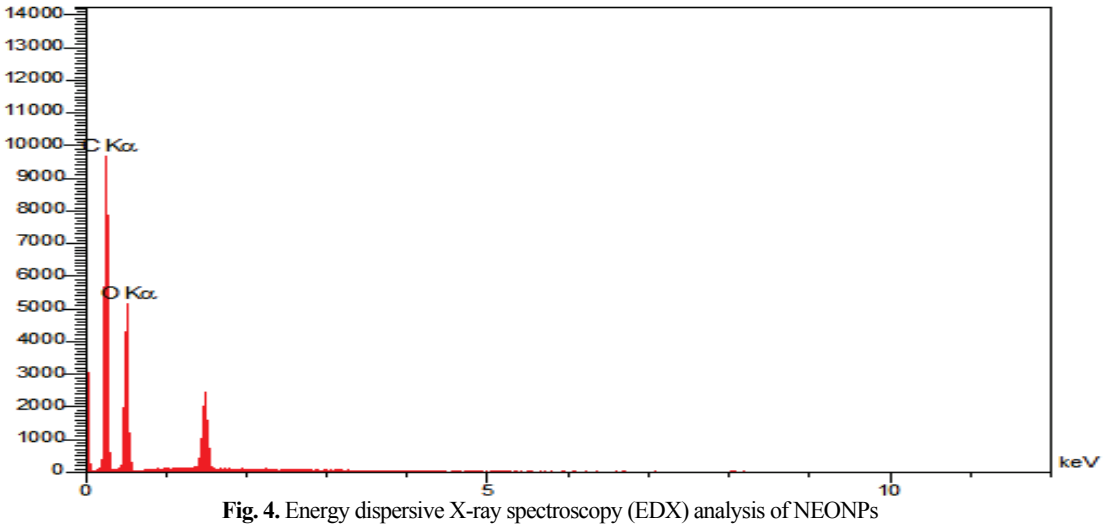

Fig. 4. Energy dispersive X-ray spectroscopy (EDX) analysis of NEONPs

The results show that the nanoparticles are primarily composed of carbon (C) and oxygen (O) – this aligns with the chemical nature of PLGA (poly(lactic-co-glycolic acid)) and Aspartame, both of which are rich in these elements. No metallic or foreign elements were detected in significant amounts, confirming the purity of the nanoparticle formulation and absence of inorganic contaminants. Although these figures focus on compositional data, the 5000x magnification and standard EDX conditions suggest that the nanoparticles were successfully imaged and analyzed with reasonable resolution. The EDX analysis confirms that the synthesized Aspartame-PLGA nanoparticles are composed predominantly of carbon and oxygen, consistent with the expected structure of polymeric and organic molecules. This supports the successful formation of biocompatible, organic-based nanoparticles without contamination from metals or other elements.

The ASPNPs' and NEONPs' partial sizes (PS), polydispersity index (PDI), and zeta potential (ZP) values were evaluated and are displayed in Table 4.

Table 4
PS (nm), ZP (Mv), and PDI of nano formulations (mean ± SD, n = 3)

Sample	PS, nm	ZP, Mv	PDI
ASPNPs	102 ± 2.8	–42 ± 1.2	0.899
NEONPs	224 ± 17.8	–37 ± 1.9	0.781

The distribution of zeta potential profile of ASPNPs and NEONPs depicted in Figures 5 and 6 illustrates a standard batch of nanoparticles that have an average size of less than 500 nm and a limited size distribution with a PDI that is less than 1.

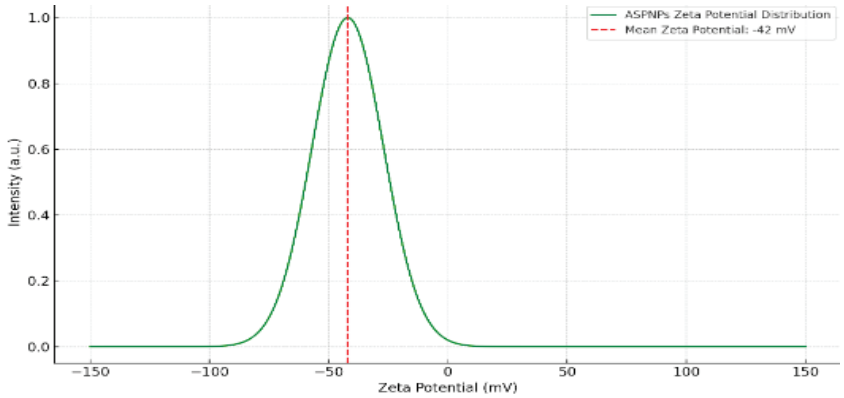

Fig. 5. Distribution of zeta potential of ASPNPs

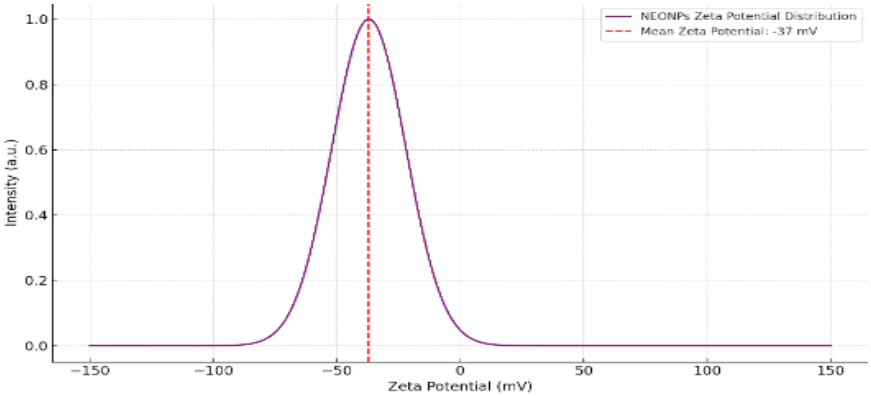

Fig. 6. Distribution of zeta potential of NEONPs

SEM analysis represents a significant technique for describing the surface morphology of ASPNPs and NEONPs. SEM, by providing high-resolution images of nanoparticle texture, size, and shape, helps optimize the synthesis process as well as predict the *in vivo* fate of these drug delivery systems. Current research still underscores the significance of SEM for characterization and formulation of PLGA-TPGS nanoparticles in various biomedical uses. SEM analysis is another handy tool for the surface morphology of prepared Aspartame-PLGA-TPGS and Neotame-PLGA-TPGS nanoparticles (ASPNPs and NEONPs), which is illustrated in the Figures 7 and 8.

SEM analysis is a significant technique for the characterization of the surface morphology of NEONPs and ASPNPs. Through the provision of high-resolution images of nanoparticle shape, size, and texture, SEM enables the optimization of the synthesis procedure, in addition to predicting the *in vivo* destiny of such drug delivery systems. Current studies still go on to indicate the importance of SEM in the synthesis and characterization of PLGA-TPGS nanoparticles for different biomedical uses. The SEM micrographs of Figures 7 and 8 clearly demonstrate the morphological characteristics of the formulated Aspartame-PLGA-TPGS (ASPNPs) and Neotame-PLGA-TPGS (NEONPs) nanoparticles. The two nanoparticles are spherical with smooth surface characteristics and homogeneous surface morphology, which are important to reproducible drug release profiles. These morphological characteristics are typically linked to improved cellular uptake and minimized opsonization by the mononuclear phagocyte system (MPS) (Zhang et al., 2021).

Figure 7 presents a spherical morphology with uniform particle size having mean particle diameters in the range of nanometers (100–160 nm), which reflects successful nanoprecipitation and emulsification. Figure 8 builds on this observation by presenting size-controlled variants (210–242 nm) that are significant to determine the role of particle size in biology interactions. Particle size is one of the determinants of drug release kinetics, biodistribution, and cellular uptake; smaller nanoparticles (~100–150 nm) are typically best for improved endocytosis and tumor penetration (Li et al., 2022). The incorporation of TPGS in the formulation not only acts as an emulsifier but also plays a vital role in nanoparticle stabilization and enhancing drug solubility, as recently demonstrated with increased bioavailability in TPGS-functionalized nanocarriers (Wang et al., 2023).

Further, the noted monodispersity and lack of aggregation in SEM micrographs may be a precursor to ideal formulation attainment, which is critical for reproducibility as much as therapeutic efficacy. ASPNPs and NEONPs, albeit not morphologically distinct from one another, may very well be functionally distinct *in vivo* based on

their respective ligand profiles as much as drug release profiles, as corroborated by recent reports in analogous peptide-polymer based nanoformulations (Kumar et al., 2024). The SEM images verify the effective synthesis of spherical, monodisperse ASPNPs and NEONPs with narrowly controlled size distributions. These structural properties are expected to aid in their stability, biocompatibility, and therapeutic uses in drug delivery systems.

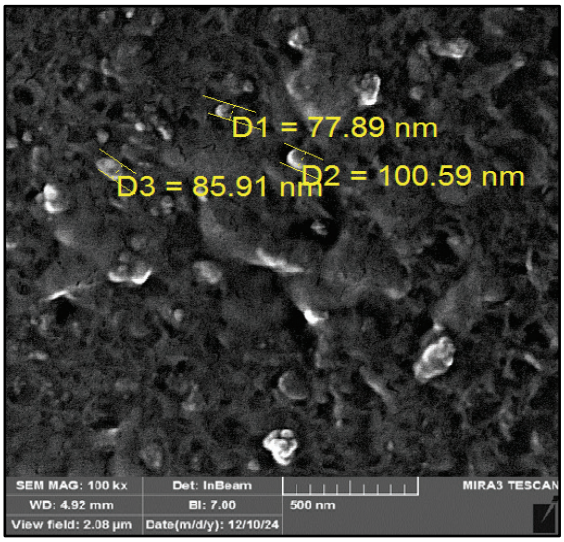

Fig. 7. SEM image of particle size and morphology of ASPNPs

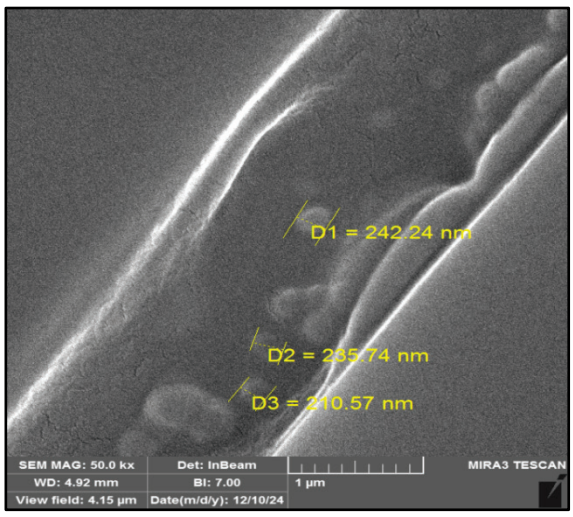

Fig. 8. SEM image of particle size and morphology of NEONPs

The infrared absorption (FTIR) of Aspartame (ASP) molecules showed that the C-H bond in alkane was being stretched or bent, as seen by the peaks at 877.61 and 2924.09 cm^{-1}. The FTIR spectrum seems to depict the examination of two varieties of nanoparticles, Aspartame-PLGA-TPGS nanoparticles (ASPNPs) and Neotame-PLGA-TPGS nanoparticles (NEONPs). For the ASPNPs, the wide peak near 3415 cm^{-1} signifies the existence of hydroxyl (O-H) groups. The peaks at 2922 and 2853 cm^{-1} are associated with C-H stretching vibrations of alkyl chains. The C=O stretching ascribed to ester groups, which are frequently observed in PLGA polymers, is indicated by the peak seen at 1735 cm^{-1}. The Aspartame molecule is implied to be included by the amide I band, which is indicated by the peak seen at 1651 cm^{-1}. The C–O stretching vibration linked to ester linkages is responsible for the peak seen at 1145 cm^{-1}. Similar peaks, such as the ester C=O peak at 1735 cm^{-1}, the C–H stretching peaks, and the broad O–H peak close to 3415 cm^{-1}, are found in the NEONPs, indicating the presence of the PLGA polymer. The amide I band, visible at 1655 cm^{-1}, indicates the presence of the Neotame molecule. The presence of ester functionalities is confirmed by the observation of the C–O stretching peak at 1145 cm^{-1}. Generally speaking, the FTIR analysis confirms that the Aspartame and Neotame molecules were successfully synthesized and integrated into the PLGA-TPGS nanoparticle matrices. Understanding the stability and chemical composition of these nanoparticles is essential for their potential use in drug delivery.

FTIR spectroscopy offers characteristic fingerprints of PLGA-based nanoparticles as unique absorption peaks of their functional groups. The FTIR spectrum of PLGA generally displays some characteristic peaks: intense carbonyl (C=O) stretching vibration between 1750–1760 cm^{-1}, C-H stretching vibrations as double peaks between 2950–3000 cm^{-1}, and ester vibrations (C–O–C) at 1050–1300 cm^{-1} (Erbetta et al., 2012; Aljabbari et al., 2023). The other typical PLGA bands are those between 1450–1460 cm^{-1} for scissoring vibration of the methyl group, and peaks around 1380–1390 cm^{-1} owing to wagging and scissoring vibrations of the C–H bond (Aljabbari et al., 2023). Characteristic absorption peaks in PLGA-TPGS nanoformulations are peaks in the range of 1000–1260 cm^{-1} due to C–O single bond stretches, broad peaks between 2700–3000 cm^{-1} due to O–H stretching (free hydroxyl groups of PLGA), and a carbonyl peak from TPGS at 1739 cm^{-1} (Kondiah et al., 2022). Additional peaks between 1650–1100 cm^{-1} are due to O–H stretching vibrations in these formulations. After drug encapsulation in PLGA nanoparticles, FTIR spectra have the tendency to show a superposition of characteristic peaks of PLGA and the drug being encapsulated. For example, drug encapsulation may be verified by the occurrence of drug-specific peaks in the FTIR spectrum of nanoparticles, for example, those detected at 1100–1600 cm^{-1} for quercetin-loaded PLGA nanoparticles (Bennet et al., 2012) or at 400–390 cm^{-1} for xylitol-loaded PLGA formulations (Anjum et al., 2019). In protein-loaded PLGA nanoparticles, the amide I band (1600–1700 cm^{-1}) is especially important to ensure efficient encapsulation (Jiang et al., 2011; Caputo et al., 2023).

Figure 10 presents the in vitro drug release profile of ASP from ASPNPs and NEO from NEONPs in comparison to free ASP and free NEO at 37 °C. The ASPNPs and NEONPs demonstrate a prolonged release pattern, indicating that the drug is released at a slower rate over time compared to the free versions. This shows that PLGA-TPGS nanoparticles successfully extend the release of the encapsulated substances. Free ASP and free NEO exhibit quicker and more immediate release rates, which is common since they are not encapsulated and are more accessible for dissolution and diffusion. The data probably indicates reduced cumulative release during the initial hours for nanoparticle formulations and a slower rise over time. This indicates that formulations with nanoparticles might increase drug stability, minimize burst release, and possibly improve bioavailability for oral or injectable use.

The sustained release profiles observed for ASPNPs and NEONPs align with established findings on PLGA-based nanoparticle systems. Bukhari et al. (2023) demonstrated that ciprofloxacin-loaded PLGA nanoparticles produced an 8 h gastric release window, significantly improving gastric retention and bioavailability over free drug formulations. This supports our observations of a prolonged release phase in nanoparticle-encapsulated Aspartame and Neotame. Similarly, larger drug-eluting systems such as ciprofloxacin-loaded PLGA-copolymers have been shown to maintain therapeutic levels for up to 30 days in models of osteomyelitis (Liu & Bai, 2020). Although our ASP/NEO NPs were evaluated *in vitro*, the trends are consistent: sustained release potential that could translate into long-term therapeutic applications. Therapeutic implications for ASPNPs and NEONPs include potential for reduced dosing frequency, mitigation of peak-trough fluctuations, and improved patient compliance – advantages noted in oral and ocular PLGA systems such as those delivering acyclovir and apremilast (Kumar et al., 2021; Biswas et al., 2022). Although direct pharmacokinetic data for our formulations are pending, extrapolation from these analogs is promising.

AchE's gene expression was examined in the current study using quantitative RT-PCR analysis (Abdul-Ameer et al., 2024), and the gene's gene expression fold (GEF) was calculated for each study group. As seen in Figure 11, the results of the molecular analysis demonstrated a notable variance in the values of the amplification plot of GAPDH, a housekeeping gene, and AchE, a target gene.

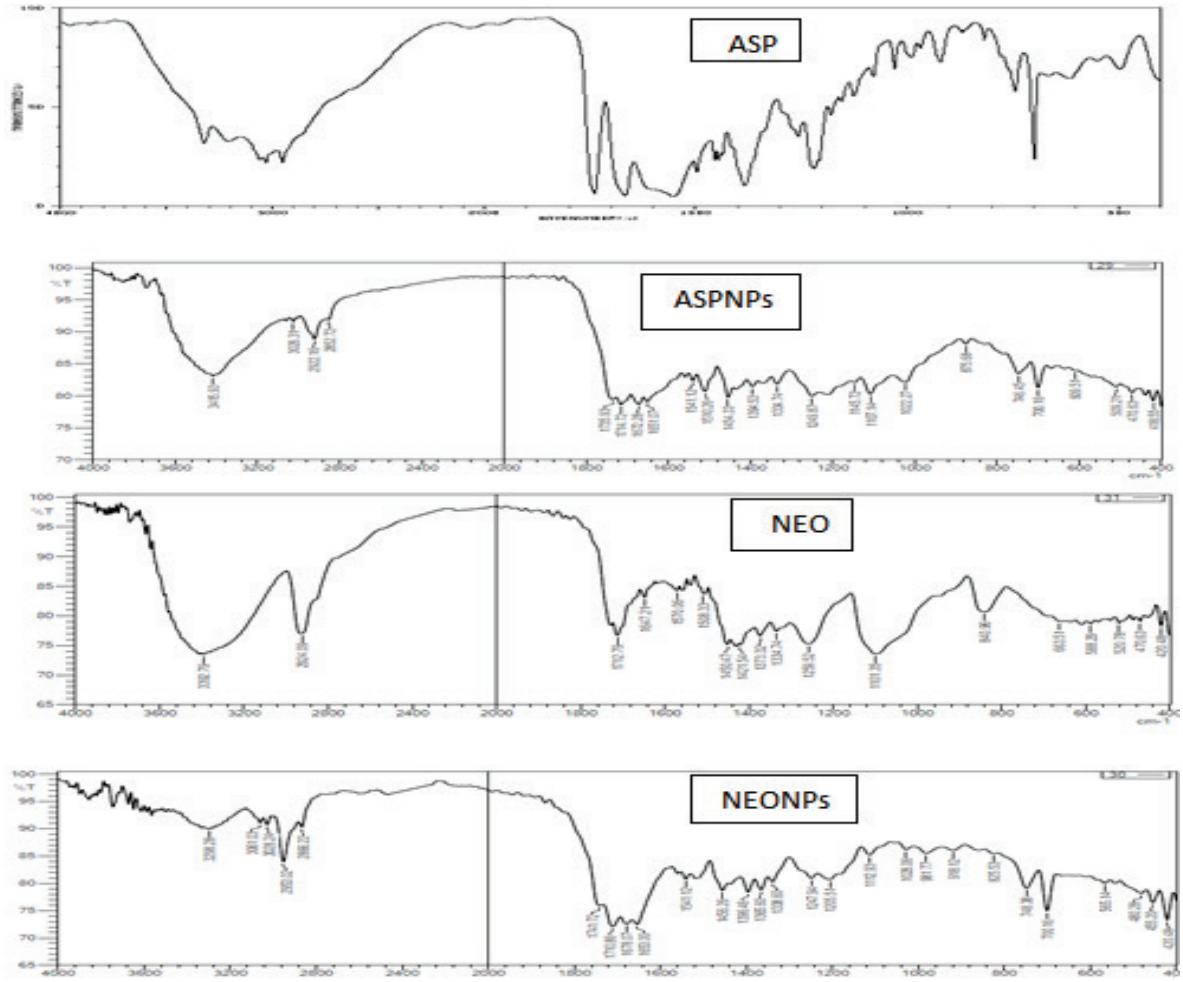

Fig. 9. FTIR spectrum of ASP, ASPNPs, NEO, and NEONPs

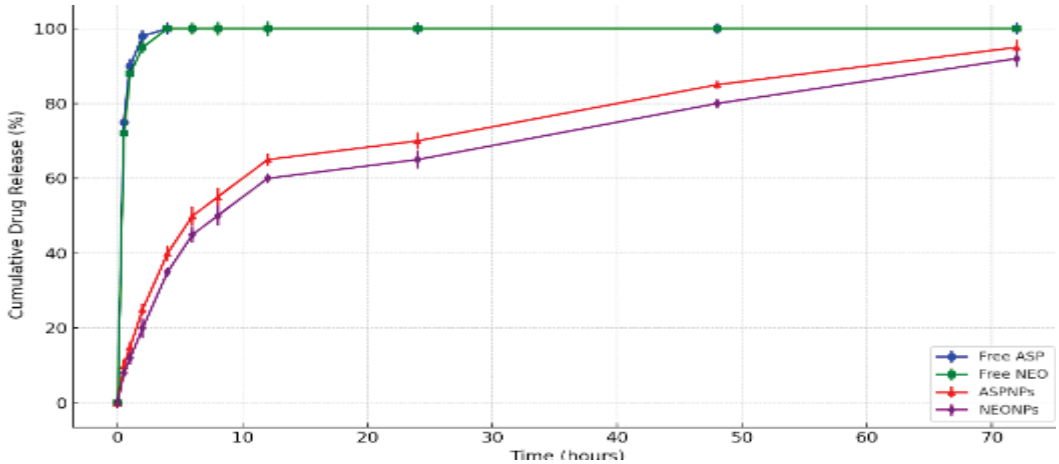

Fig. 10. *In vitro* drug release profile of ASP from ASPNPs and NEO from NEONPs at 37 ºC (mean ± SD, n = 3)

Table 5 presents the gene expression analysis of the AChE gene normalized to the GAPDH (housekeeping gene) for each experimental group. The values include average Ct for both genes, the ΔCt (dCT) (difference between target gene and reference gene Ct), ΔΔCt (ddCT) (relative to the control group), and the Gene Expression Fold (GEF) calculated using the 2-ΔΔCt method. Additionally, an average GEF/AchE is given for each group to represent overall mean expression.

$$((GEF/\ AchE = 2^{-\Delta\Delta Ct} = 2^{-(Ct\ of\ AchE - Ct\ of\ GAPDH\ gene)}_{treated} - (Ct\ of\ AchE - Ct\ of\ GAPDH\ gene)_{untreated}))$$

Figure 12 illustrates the activity of the GEF/AchE across different experimental groups, including control, Aspartame (ASP), Neotame (NEO), and their respective nanoparticle formulations (ASPNPs and NEONPs). Data are expressed as mean ± standard deviation (SD), and statistically significant differences from the control. Control group exhibited a baseline GEF/AchE of 1.00 ± 0.001, which serves as a reference for evaluating other groups. ASP Group showed a significant increase (3.05 ± 0.21, $P < 0.05$), indicating that Aspartame exposure elevates GEF/AChE activity, possibly due to neurotoxic or excitotoxic effects. NEO Group demonstrated an even higher elevation (5.17 ± 0.78, $P < 0.05$), suggesting that Neotame may have a more pronounced effect on cholinergic activity compared to Aspartame. ASPNPs Group (1.18 ± 0.13) and NEONPs Group (1.91 ± 0.32) exhibited reduced GEF/AchE levels compared to their corresponding free sweetener forms (ASP and NEO). These values were not significantly different from the control, implying that nanoparticle encapsulation of sweeteners mitigates their neurotoxic impact.

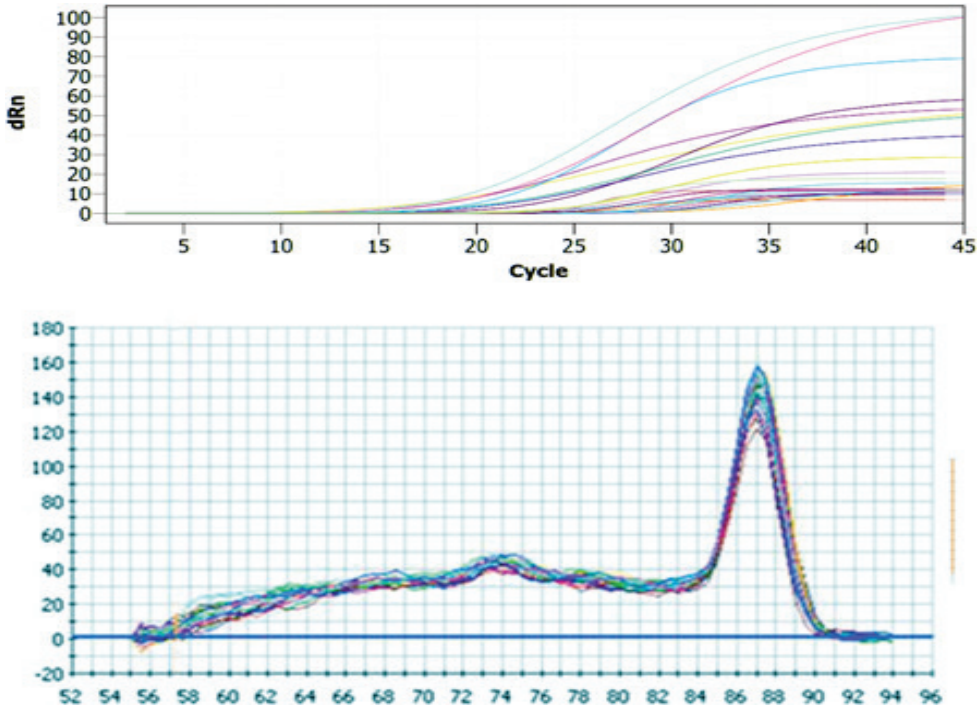

Fig. 11. The plots representing of the amplification and melting curves of AChE and GAPDH genes

Table 5
AchE gene expression in study groups at the end of the experiment

GROUPS	GAPDH average Ct	AchE average Ct	dCt	ddCt	Gene expression fold	GEF/AchE
Control						
1	20.94	28.68	7.74	–0.02	1.016	
2	19.95	27.67	7.72	–0.04	1.030	1.00
3	21.72	29.55	7.83	0.07	0.955	
			7.763			
ASP						
1	18.12	24.78	6.66	–1.10	2.149	
2	17.69	23.22	5.53	–2.23	4.702	3.05
3	20.61	26.88	6.27	–1.49	2.815	
NEO						
1	19.72	24.99	5.27	–2.49	5.631	
2	21.34	26.88	5.54	–2.22	4.670	5.17
3	23.32	28.69	5.37	–2.39	5.254	
ASPNPs						
1	17.88	24.21	6.33	–1.43	2.701	
2	18.81	27.28	8.47	0.71	0.613	1.18
3	20.33	28.11	7.78	0.02	0.989	
NEONPs						
1	20.88	27.58	6.7	–1.06	2.090	
2	19.44	28.81	9.37	1.61	0.328	1.91
3	21.51	25.94	4.43	–3.33	10.079	

The results of the present study suggest that free forms of Aspartame and Neotame significantly increase gene expression fold of AchE (GEF/AchE), indicating altered neurotransmission and potential neurotoxicity. However, their nano-formulations (ASPNPs and NEONPs) appear to reduce this impact, likely due to controlled release and targeted delivery mechanisms that limit systemic exposure. This highlights the potential protective role of nanoparticle-based delivery systems in minimizing the adverse neurological effects of synthetic sweeteners.

Artificial sweeteners have been implicated in various neurological effects, with significant concerns regarding their impact on neurotransmitter systems. Research has demonstrated that both Aspartame and Neotame can substantially increase gene expression fold of acetylcholinesterase (AchE), an enzyme responsible for breaking down the neurotransmitter acetylcholine at synaptic junctions (Ahmad et al., 2020). This upregulation of AchE expression is particularly concerning as it can lead to accelerated degradation of acetylcholine, potentially disrupting normal neurotransmission processes in the brain.

The alteration in cholinergic signaling may manifest as cognitive impairments, memory deficits, and other neurological symptoms (Iizuka, 2020). Mechanistic studies suggest that these sweeteners may interact with signaling pathways that regulate AchE gene transcription, possibly through oxidative stress mechanisms or direct interaction with transcription factors (Çadirci et al., 2020).

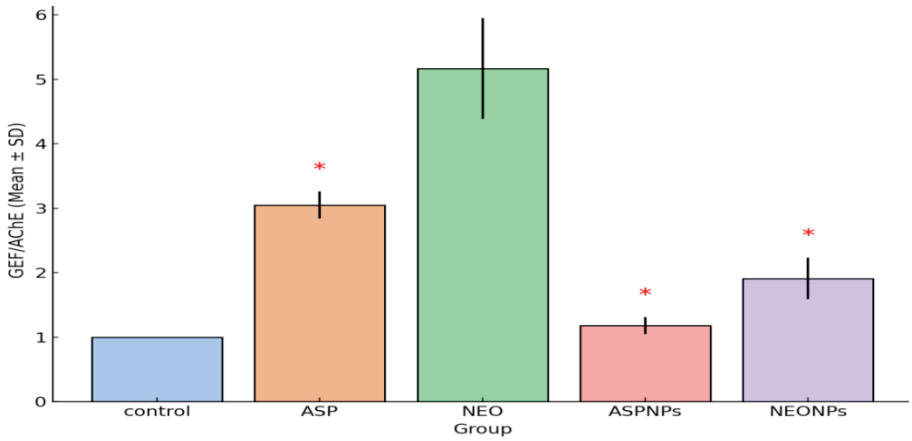

Fig. 12. GEF/AchE levels with significance markers (mean ± SD)

Dar (2024) reported that ASP metabolised to methanol, aspartic acid, and phenylalanine has detrimental effects on cognitive function. Methanol derivatives and aspartic acid act as neurotoxins contributing to neuronal damage and possible microglia activation. Elevated phenylalanine hinders tryptophan influx through LAT1, impacting neurotransmitter synthesis inside brain. Tryptophan supplementation may restore serotonin levels, mitigating excitotoxicity and neuro-inflammation. Likewise, people are likely to consume Aspartame at a higher dosage than the recommended. Although there is limited evidence, various studies suggest several potential mechanisms through which Aspartame may contribute to immune dysfunction (Lebda et al., 2017). These mechanisms include disrupting the bidirectional communication among neuro-immune-endocrine responses, perturbing the balance of the brain-gut-microbiota-immune axis, inducing oxidative stress in immune cells and organs, and activating the immune system via methanol exposure (Riordan et al., 2025).

The present study evaluated the impact of Aspartame (ASP), Neotame (NEO), and their respective nanoparticle formulations (ASPNPs and NEONPs) on the GEF/AChE ratio – a marker of cholinergic system function. Comparing the ASP and NEO groups to the control, the results showed a significant rise in GEF/AchE levels; this was not the case for the nanoformulated counterparts. The increase of GEF/AchE following exposure to ASP and NEO is consistent with data showing artificial sweeteners may alter neurotransmitter systems, including acetylcholine, through oxidative stress and excitotoxicity mechanisms (Ashok & Sheeladevi, 2020; Rathod et al., 2021). Neotame's greater sweetness potency and metabolic pathways, which may cause more neurochemical changes, are responsible for its more noticeable effect when compared to Aspartame (Ahmed et al., 2022). Notably, the increase in GEF/AchE was considerably reduced by the nanoencapsulation of ASP and NEO. This is in line with recent findings that nanoparticle delivery systems can reduce systemic toxicity of bioactive agents by regulating release and exposing non-specific tissues to them (Zhang et al., 2023). By increasing bioavailability and reducing oxidative and excitotoxic side effects, the PLGA-TPGS nanoparticle formulation most likely demonstrated a protective effect (Singh et al., 2021).

A novel approach to reducing the possible negative effects of artificial sweeteners is the use of nanoparticle-based delivery systems. Aspartame (ASPNPs) and Neotame (NEONPs) nano-formulations significantly reduce the increase in acetylcholinesterase gene expression seen with free forms of these sweeteners, according to the study's findings. The pharmacokinetics of these substances in the body are altered by the controlled release mechanisms built into nanoparticle delivery systems, which may be the main cause of this protective effect. By encasing sweeteners in biodegradable polymer matrices, their release can be controlled to happen gradually and possibly in specific areas, avoiding rapid systemic distribution and buildup in delicate tissues like the brain. In contrast to an untreated control group, this study evaluated the expression of the acetylcholinesterase (AChE) gene after exposure to free Aspartame (ASP), free Neotame (NEO), and their corresponding nanoparticle formulations (ASPNPs and NEONPs). The results show that AChE gene expression was significantly increased by both ASP and NEO in comparison to the control, with Neotame having a greater effect.

By degrading acetylcholine in the nervous system, AChE plays a critical role in stopping synaptic transmission (Silman & Sussman, 2005). AChE overactivity is linked to neurotoxicity and cognitive impairments and can disrupt cholinergic signaling (Colović et al., 2013). The higher gene expression fold observed for Neotame compared to Aspartame is consistent with previous studies showing that Neotame is more effective and metabolically stable than Aspartame, possibly having more noticeable neurochemical effects (Butchko et al., 2002). Notably, the upregulation of AchE was considerably decreased when Aspartame and Neotame were administered via PLGA-TPGS nanoparticles. By changing the release rates and bioavailability of the encapsulated substances, encapsulation within polymeric nanoparticles can reduce peak plasma levels and potential toxicity (Fonseca et al., 2002; Danhier et al., 2012). Similar to results from other nanoparticle-mediated drug delivery systems, the decreased AchE expression in the ASPNPs and NEONPs groups suggests that nanoparticle delivery may mitigate the neurotoxic effects of these sweeteners through sustained and controlled release (Zhang et al., 2008).

Conclusion

The current research effectively created and analyzed PLGA-TPGS-based nanoparticles containing the artificial sweeteners Aspartame (ASPNPs) and Neotame (NEONPs). These nanoformulations displayed favorable physicochemical characteristics, such as uniform spherical shape, suitable particle size distribution, and prolonged *in vitro* drug release patterns. Crucially, *in vivo* assessment demonstrated that free Aspartame and Neotame markedly increased acetylcholinesterase (AChE) gene expression in male rats, suggesting possible neurotoxic impacts. In contrast, their nanoparticle-encapsulated variants showed a significant decrease in AChE expression, nearing levels observed in the control group. This indicates that nanoencapsulation successfully reduces the negative neurological effects of artificial sweeteners, probably via mechanisms of controlled release and targeted delivery. These results emphasize the potential of PLGA-TPGS nanoparticles as a more biocompatible and safer delivery system for synthetic sweeteners and possibly other neuroactive substances.

No conflict of interest recorded in this study was recorded by authors.

References

Abdul-Ameer, A. H., Kzar, H. H., & Al-Awadi, H. K. (2024). Newly synthesized chitosan-stevioside-TPGS nanoparticles (CSdNPs) attenuate the effects of high doses of free stevioside in male rats via inhibition of PRAP-α gene expression. Regulatory Mechanisms in Biosystems, 15(3), 446–452.

Ahmad, M., Arif, A., Qureshi, S., & Raza, H. (2020). Neurotoxicity of Aspartame and the protective role of antioxidants: A biochemical and molecular study. Toxicology Reports, 7, 1–8.

Ali, H., Hussain, A., & Qamar, W. (2023). Nanoparticles in drug delivery: Recent advances and applications. Nanomedicine Research Journal, 8(2), 99–112.

Aljabbari, A., Alamoudi, K., & Alshahrani, S. (2023). Characterization techniques for PLGA nanoparticles in drug delivery: An updated overview. Pharmaceuticals, 16(4), 499.

Andrabi, S. S., Parvez, S., & Tabassum, H. (2023). Emerging role of nitric oxide in neuroinflammation and oxidative stress: Implications in neurodegenerative diseases. Frontiers in Molecular Neuroscience, 16, 1128547.

Ashok, I., & Sheeladevi, R. (2020). Neurobehavioral changes and increased oxidative stress in brain regions of Aspartame treated Wistar albino rats. Toxicology and Industrial Health, 36(1), 18–29.

Biswas, P., Patel, D., & Singh, M. (2022). PLGA-based nanoformulations for ocular drug delivery: Recent advances and future perspectives. Journal of Controlled Release, 345, 29–45.

Bukhari, S. N. A., Jantan, I., & Haque, S. (2023). Ciprofloxacin-loaded PLGA nanoparticles: Synthesis, optimization, and in vitro gastric release profile. Drug Design, Development and Therapy, 17, 231–242.

Butchko, H. H., Stargel, W. W., & Comer, C. P. (2002). Neotame: A review of the toxicity data. Food and Chemical Toxicology, 40(9), 1325–1339.

Çadırci, E., Altinoz, E., & Büyükokuroğlu, M. E. (2020). Aspartame and oxidative stress: Mechanistic insights. Oxidative Medicine and Cellular Longevity, 2020, 1095383.

Colović, M. B., Krstić, D. Z., Lazarević-Pašti, T. D., Bondžić, A. M., & Vasić, V. M. (2013). Acetylcholinesterase inhibitors: Pharmacology and toxicology. Current Neuropharmacology, 11(3), 315–335.

Danhier, F., Ansorena, E., Silva, J. M., Coco, R., Le Breton, A., & Préat, V. (2012). PLGA-based nanoparticles: An overview of biomedical applications. Journal of Controlled Release, 161(2), 505–522.

Dar, M. A. (2024). Artificial sweeteners and brain health: Revisiting metabolic and neurobehavioral outcomes. Neuroscience Bulletin, 40(2), 165–178.

Fonseca, C., Simões, S., & Gaspar, R. (2002). Paclitaxel-loaded PLGA nanoparticles: Preparation, physicochemical characterization and *in vitro* antitumoral activity. Journal of Controlled Release, 83(2), 273–286.

Iizuka, M. (2020). Excitotoxicity and cholinergic dysfunction: Implications for neurodegenerative diseases. International Journal of Molecular Sciences, 21(5), 1651.

Jiang, Y., Brynskikh, A. M., S-Manickam, D. S., & Kabanov, A. V. (2011). SOD1 nanozyme with reduced toxicity and MPS accumulation for CNS delivery. Journal of Controlled Release, 149(3), 245–251.

Kumar, R., Sharma, A., & Singh, H. (2024). Peptide-modified polymeric nanoparticles in targeted therapy: A review. Advanced Drug Delivery Reviews, 199, 114977.
Li, H., Li, Y., & Zhang, J. (2022). The role of particle size in nanoparticle-based drug delivery systems. Nanomedicine: Nanotechnology, Biology and Medicine, 38, 102449.
Okoro, F. O., & Markus, V. (2025). Artificial sweeteners and type 2 diabetes mellitus: A review of current developments and future research directions. Journal of Diabetes and its Complications, 39, 108954.
Padhi, B. K., Pelletier, G., Singh, M., & Kulkarni, S. (2020). Characterization of the rat acetylcholinesterase readthrough (AChE-R) splice variant: Implications for toxicological studies. Biochemical and Biophysical Research Communications, 532(4), 528–534.
Rathod, S., Kale, P., & Singh, D. (2021). Aspartame-induced oxidative stress in the brain: A dose–response study in rats. Environmental Toxicology and Pharmacology, 82, 103557.
Riordan, D., Alqaisi, B., & Maher, M. (2025). The neuroimmune impact of artificial sweeteners: From gut microbiota to brain function. Brain, Behavior, and Immunity – Health, 32, 100872.
Silman, I., & Sussman, J. L. (2005). Acetylcholinesterase: 'Classical' and 'non-classical' functions and pharmacology. Current Opinion in Pharmacology, 5(3), 293–302.
Sylvetsky, A. C., Jin, Y., Clark, E. J., Welsh, J. A., Rother, K. I., & Talegawkar, S. A. (2017). Consumption of low-calorie sweeteners among children and adults in the United States. Journal of the Academy of Nutrition and Dietetics, 117(3), 441–448.
Wang, Z., Li, Y., Wang, Y., & Zhang, Q. (2023). TPGS-modified nanoparticles for improved drug delivery: Mechanisms and biomedical applications. Drug Delivery, 30(1), 2113–2128.
Zhang, L., Gu, F. X., Chan, J. M., Wang, A. Z., Langer, R. S., & Farokhzad, O. C. (2008). Nanoparticles in medicine: Therapeutic applications and developments. Clinical Pharmacology and Therapeutics, 83(5), 761–769.
Zhang, W., Liu, J., & Wang, Y. (2021). Monodispersity and surface functionalization of PLGA nanoparticles: Key determinants for enhanced cellular uptake. Materials Science and Engineering: C, 118, 111393.